Virus Research 153 (2010) 82–91

Contents lists available at ScienceDirect

Virus Research

journal homepage: www.elsevier.com/locate/virusres

Mapping of amino acid residues responsible for adhesion of cell culture-adapted foot-and-mouth disease SAT type viruses

Francois F. Maree[a,*], Belinda Blignaut[a,b], Tjaart A.P. de Beer[c,1], Nico Visser[d], Elizabeth A. Rieder[e]

[a] Transboundary Animal Diseases Programme, Onderstepoort Veterinary Institute, Agricultural Research Council, Onderstepoort 0110, South Africa
[b] Department of Microbiology and Plant Pathology, Faculty of Agricultural and Natural Sciences, University of Pretoria, Pretoria 0002, South Africa
[c] Bioinformatics and Computational Biology Unit, University of Pretoria, Pretoria 0002, South Africa
[d] Intervet/Schering-Plough, Boxmeer 5830AA31, The Netherlands
[e] Foreign Animal Disease Research Unit, United States Department of Agriculture, Agricultural Research Service, Plum Island Animal Disease Center, Greenport, NY 11944, USA

ARTICLE INFO

Article history:
Received 29 March 2010
Received in revised form 6 July 2010
Accepted 8 July 2010
Available online 15 July 2010

Keywords:
Chimera
Foot-and-mouth disease virus
Glycosaminoglycan
Heparan sulfate proteoglycan
Cell receptor

ABSTRACT

Foot-and-mouth disease virus (FMDV) infects host cells by adhering to the α_V subgroup of the integrin family of cellular receptors in a Arg–Gly–Asp (RGD) dependent manner. FMD viruses, propagated in non-host cell cultures are reported to acquire the ability to enter cells via alternative cell surface molecules. Sequencing analysis of SAT1 and SAT2 cell culture-adapted variants showed acquisition of positively charged amino acid residues within surface-exposed loops of the outer capsid structural proteins. The fixation of positively charged residues at position 110–112 in the βF–βG loop of VP1 of SAT1 isolates is thought to correlate with the acquisition of the ability to utilise alternative glycosaminoglycan (GAG) molecules for cell entry. Similarly, two SAT2 viruses that adapted readily to BHK-21 cells accumulated positively charged residues at positions 83 and 85 of the βD–βE loop of VP1. Both regions surround the fivefold axis of the virion. Recombinant viruses containing positively charged residues at position 110 and 112 of VP1 were able to infect CHO-K1 cells (that expresses GAG) and demonstrated increased infectivity in BHK-21 cells. Therefore, recombinant SAT viruses engineered to express substitutions that induce GAG-binding could be exploited in the rational design of vaccine seed stocks with improved growth properties in cell cultures.

1. Introduction

Foot-and-mouth disease (FMD) is a highly contagious vesicular disease of cloven-hoofed animals causing significant distress and suffering in animals. Although mortality is usually low (<5%) (Thomson, 1995), morbidity can reach 100% and the impact can be catastrophical when an outbreak occurs in a FMD-free region with immunologically naïve population of livestock. Consequently FMD is classified by the OIE as one of the most important infectious diseases of livestock (Office International des Épizooties Terrestrial Manual, 2009). The economically critical effects to livestock farming due to the high cost of disease control and international trade restrictions (Sellers and Daggupaty, 1990) was evidenced during the 2000–2001 outbreaks in Europe and the virus escape that occurred more recently, in 2007 in the United Kingdom (Samuel and Knowles, 2001; Cottam et al., 2008). In endemic regions, FMD is controlled by restricting animal movement, the implementation of vaccination programmes and biosecurity measures. In disease-free countries where vaccination is normally not applied, ring-vaccination is only used in an emerging outbreak with subsequent slaughtering of vaccinated animals (Müller et al., 2001; Tomassen et al., 2002).

In South Africa, other regions of the African continent, as well as in some Asian and South American countries, regular immunisation is essential for disease control, and in maintaining FMD-free status. Current FMD vaccines are chemically inactivated preparations of concentrated, virus-infected cell culture supernatants (Office International des Épizooties Terrestrial Manual, 2009). Therefore, large-scale vaccine production utilize a suitable cell line, like BHK-21 cells, and requires that the vaccine strain is adapted and propagated in cell culture (Amadori et al., 1994, 1997). However, these cell lines have limited (monolayers) or no (in suspension) expression of the required primary receptor for infection by FMDV

Abbreviations: FMD, foot-and-mouth disease; FMDV, FMD virus; GAG, glycosaminoglycan; HSPG, heparan sulfate proteoglycan; SAT, South African Territories.

* Corresponding author at: Transboundary Animal Diseases Programme, Onderstepoort Veterinary Institute, Private Bag X05, Onderstepoort 0110, South Africa. Tel.: +27 12 529 9560/85; fax: +27 12 529 9505.
E-mail address: Mareef@arc.agric.za (F.F. Maree).
[1] Currently at: European Bioinformatics Institute, Wellcome Trust Campus, Hinxton, Cambridge, CB10 1SD, United Kingdom.

0168-1702/$ – see front matter © 2010 Elsevier B.V. All rights reserved.
doi:10.1016/j.virusres.2010.07.010

(Amadori et al., 1994). In the early 1980s it was noted that viruses of the three SAT serotypes, endemic in Africa, are notorious for their difficulty to adapt to BHK-21 cells (Pay et al., 1978; Preston et al., 1982). It is thought that the cell surface molecules, which may act as virus receptors, exert an important selective pressure on viral RNA quasi-species, thereby enabling adaptation. Studies have shown that repeated passaging of FMDV in cultured cells rapidly gave rise to mutant viruses within the population (Rieder et al., 1994; Herrera et al., 2007). Adaptation of wild-type SAT viruses in cell culture to produce high yields of stable antigen is an intricate and time-consuming process that is often associated with a low success rate.

FMD virus (FMDV), the type species of the *Aphtovirus* genus in the family *Picornaviridae* (Racaniello, 2006), infects epithelial cells by adhering to any of four members of the α_V subgroup of the integrin family of cellular receptors, *i.e.* $\alpha_V\beta1$, $\alpha_V\beta3$, $\alpha_V\beta6$ and $\alpha_V\beta8$ (Berinstein et al., 1995; Neff et al., 1998, 2000; Jackson et al., 1997, 2000, 2002, 2004; Duque and Baxt, 2003). Attachment to the receptors is mediated via a highly conserved Arg–Gly–Asp (RGD) motif (Fox et al., 1989; Baxt and Becker, 1990; Mason et al., 1994; Leippert et al., 1997) located within the structurally disordered βG–βH loop of VP1 (Acharya et al., 1989; Lea et al., 1995; Curry et al., 1997). Following FMDV–receptor interactions, the virus is internalised and the viral genome is released in the cytosol. Adaptation of FMD field isolates to enable efficient replication in cultured cells is accompanied by changes in viral properties, including the acquisition of the ability to bind to alternative cellular receptors such as cell surface glycosaminoglycans (GAGs) (Jackson et al., 1996, 2001; Sa-Carvalho et al., 1997; Zhao et al., 2003). The interactions of a diverse group of ligands, such as growth factors, chemokines, herpes simplex virus (HSV), human immunodeficiency virus, respiratory syncytial virus, alphaviruses, dengue virus, adeno-associated virus and FMDV, to the highly sulfated GAGs (also known as heparan sulfate proteoglycans, HSPG) is typically via a positively charged domain on these proteins (Patel et al., 1993; Gromm et al., 1995; Jackson et al., 1996; Chen et al., 1997; Krusat and Streckert, 1997; Sa-Carvalho et al., 1997; Byrnes and Griffin, 1998; Klimstra et al., 1998; Summerford and Samulski, 1998; Fry et al., 1999, 2005; Zhao et al., 2003). The ability of a type O virus to enter cells following adhesion to HSPG is thought to be dependent on the presence of the positively charged Arg residue at position 56 of VP3 which results in a net gain of positive charge on the virion surface (Sa-Carvalho et al., 1997; Fry et al., 1999).

Replacement of the external capsid-coding sequence of an infectious cDNA clone with the corresponding region of an outbreak virus results in the transfer of surface-exposed epitopes from the aetiological agent to the recombinant virus (Zibert et al., 1990; Rieder et al., 1993; Almeida et al., 1998; Van Rensburg and Mason, 2002; Van Rensburg et al., 2004). The chimeric viruses, produced in this manner, induce a protective immune response in animals similar to that of the outbreak virus. However, co-transferral of undesirable traits, such as capsid instability and poor cell culture adaptation of the field virus may also occur. Therefore, application of reverse genetics technology in FMD vaccinology includes the identification of amino acid sequences associated with the acquisition of HSPG-binding during cell culture adaptation of SAT viruses and the introduction of these changes into chimeric constructs.

In this report we identify novel amino acid residues within the capsid proteins of SAT1 and SAT2 viruses that affect the virus' ability to grow in different cell lines. We demonstrated that cell culture adaptation to BHK-21 cells is acquired following repeated passaging of the field viruses in these cells. Furthermore, we illustrated that this phenotype can be transferred to an infectious cDNA clone of a FMD field virus from which viable cell culture-adapted viruses were recovered.

2. Materials and methods

2.1. Cells, viruses and plasmids

Baby hamster kidney (BHK) cells, strain 21, clone 13 (ATCC CCL-10) were maintained as described by Rieder et al. (1993). Chinese hamster ovary (CHO) cells strain K1 (ATCC CCL-61) were maintained in Ham's F-12 medium (Invitrogen), supplemented with 10% foetal calf serum (Delta Bioproducts). Primary pig kidney (PK) and Instituto Biologico renal suino (IB-RS-2) cells Plaque assays were performed using a tragacanth overlay method and 1% methylene blue staining (Rieder et al., 1993).

Viruses used in this study included four SAT1 viruses, *i.e.* KNP/196/91, SAR/9/81, NAM/307/98 and ZAM/2/93; and four SAT2 isolates, *i.e.* ZIM/14/90, ZIM/5/83, ZAM/7/96, and KNP/19/89. The host species the viruses were isolated from is summarized in Table 1. The SAT2/ZIM/7/83 vaccine strain is a derivative of ZIM/5/83 and is used in inactivated vaccines to assist with control of FMD along the borders of South Africa. The viruses were isolated in primary pig kidney cells (PK) and grown on IB-RS-2 cells (parental viruses) prior to adaptation to BHK-21 cells (vaccine strains). To distinguish the low passage, parental viruses from their BHK-21 culture-adapted derivatives, we will refer to the field isolate by its accession code followed by P (parental) or Vac/BHK (vaccine or BHK-21 cell-adapted strain) superscript. The passage histories of the viruses are summarised in Table 1.

The construction of plasmids pSAT2, pNAM/SAT and pSAU/SAT is described elsewhere (Böhmer, 2004; Van Rensburg et al., 2004; Storey et al., 2007). In short, the pNAM/SAT and pSAU/SAT were constructed by replacing the outer capsid-coding region of pSAT2 with the corresponding region of SAT1/NAM/307/98 and SAT2/SAU/6/00 using the unique restriction sites SspI and XmaI in VP2 and 2A-coding regions, respectively (Böhmer, 2004; Storey et al., 2007).

2.2. RNA extraction, cDNA synthesis, PCR amplification and nucleotide sequencing

RNA was extracted from infected cell lysates using either a guanidium-based nucleic acid extraction method (Bastos, 1998) or TRIzol® reagent (Life Technologies) according to the manufacturer's specifications and used as template for cDNA synthesis. Viral cDNA was synthesised with SuperScript III™ (Life Technologies) and oligonucleotide 2B208R (Bastos et al., 2001). cDNA copies of the *ca.* 3.0 kb Leader/capsid-coding regions of the viral isolates were obtained by PCR amplification using AdvanTaq™ DNA polymerase (Clontech) with specific oligonucleotides (NCR2: 5′-GCTTCTATGCCTGAATAGG and WDA: 5′-GAAGGGCCCAGGGTTGGACTC) following the manufacturer's recommendations. Sequencing of the amplicons was performed using the ABI PRISM™ BigDye Terminator Cycle Sequencing Ready Reaction Kit v3.0 (PerkinElmer Applied Biosystems). The GeneBank accession numbers of the wild-type (low passage history) virus P1 sequences are as follows: DQ009715 (SAR/9/81); DQ009716 (KNP/196/91); DQ009717 (NAM/307/98); DQ009719 (ZAM/2/93); DQ009726 (ZIM/7/83); DQ009728 (ZIM/14/90); DQ009741 (ZAM/7/96); DQ009735 (KNP/19/89). The differences in deduced amino acid sequences between the wild-type and cell culture-adapted strains are summarised in Table 2.

2.3. Site-directed mutagenesis of cDNA clones

Site-directed mutagenesis of plasmids pNAM/SAT and pSAU/SAT was accomplished by using amplicon overlap site-directed mutagenesis. The forward mutagenesis primer for

Table 1
Summary of SAT1 and SAT2 viruses and their derivatives used in production, field isolate and their derivatives, passage histories, titres prior to and after adaptation and properties in cell culture.

Serotype	Viruses[a]	Host species	Passage history[b]	Vaccine stock[c]	Titre (pfu/ml) in BHK cells	CHO-K1 infectivity[d]
SAT1	KNP/196/91^{P}	Buffalo	PK_1	–	5.2×10^7	1.08×10^{-4}
	KNP/196/91^{Vac}	–	$PK_1RS_4B_1BHK_5$	MSV	1.3×10^8	2.80×10^6
	SAR/9/81^{Epi}	Impala	epithelium	–	9.6×10^7	6.40×10^{-3}
	SAR/9/81^{Vac}	–	$PK_1RS_4BHK_5$	MSV	7.2×10^9	1.10×10^6
	NAM/307/98^{P}	Buffalo	PK_1RS_1	–	–	–
	NAM/307/98^{BHK}	–	$PK_1RS_1BHK_5$	–	1.1×10^7	–
	ZAM/2/93^{P}	Buffalo	BTY_1RS_2	–	8.6×10^6	2.82×10^{-4}
	ZAM/2/93^{BHK}	–	$BTY_1RS_2BHK_5$	–	2.2×10^8	1.06×10^7
SAT2	KNP/19/89^{P}	Buffalo	$PK_1RS_1B_1$	–	2.2×10^5	1.19×10^{-5}
	KNP/19/89^{Vac}	–	$B_1PK_1RS_1BHK_4$	MSV	1.1×10^7	5.06×10^6
	ZIM/5/83^{P}	Bovine	BTY_4RS_1	–	1.8×10^5	5.91×10^{-5}
	ZIM/5/83^{BHK}	–	$BTY_4RS_2BHK_8$	–	3.4×10^7	–
	ZIM/7/83^{Vac}	Bovine	$B_1BHK_4B_1BHK_5$	MSV	1.8×10^7	6.58×10^6
	ZIM/14/90^{P}	Buffalo	BTY_1RS_3	–	1.0×10^5	–
	ZIM/14/90^{BHK}	–	$BTY_1RS_3BHK_8$	–	2.0×10^6	–
	ZAM/7/96^{P}	Buffalo	BTY_1RS_2	–	8.0×10^6	–
	ZAM/7/96^{BHK}	–	$BTY_2RS_2BHK_8$	–	5.6×10^7	–

[a] The viruses used in this study were notated by the superscript P = most primary isolate for that strain defined as the lowest passage history; Vac = vaccine strain adapted on BHK-21 for production purpose; Epi = isolate from the epithelium tissue of the host species; BHK = propagated in BHK-21 monolayers.
[b] The passage history of the primary isolates and their derivates are indicated by cell type followed by the number of passages: B = bovine; PK = primary pig kidney cells; BTY = bovine thyroid cells; RS = IB-RS-2 cells; BHK = baby hamster kidney cells (strain 21, clone 13).
[c] MSV = master seed virus.
[d] The infectivity in CHO-K1 cells is expressed as a titre difference between a 1 and 24 h post-infection of CHO-K1 cells. A negative value is indicative of inability to infect and replicate in CHO-K1 cells, whereas a positive value indicate infection and replication in the same cell line. "–" has not been done.

pNAM/SAT was CAGTCGTCTTCTCCaaacGAcGCACCACTCGCTTCGC (NAMmut4; lower cased letters represent altered bases), replacing the wild-type KGG sequence at position 110–112 of VP1 with KRR. Similarly the mutagenesis primers for pSAU/SAT were GTGGGCGACCACCggcgcGCCTTTTGGCAGCCTAAC (SAUmut1) and GTACGCTGACAGCAaGCACaaactcCCGTCAACCTTC (SAUmut2). The latter primers introduced the E85R and E161K substitutions respectively. Briefly, the first PCR reactions were performed using NAMmut4, SAUmut1 and SAUmut2 as the sense mutagenic and cDNA-2A (CGCCCCGGGGTTGGACTCAACGTCTCC; XmaI site underlined) as the antisense oligonucleotides. The second PCR reactions were performed with the reverse complements of NAMmut4, SAUmut1 and SAUmut2 as antisense mutagenic in combination with 5′-specific sense oligonucleotides, cDNA-NAM (CGGAATATTGACCACCAGCCATGGTACCACCAC; SspI site underlined) or cDNA-SAU (CGGAATATTGACCACACGTCACGGAACCACGAC; SspI site underlined). Cycling conditions for both PCRs were as follows: 95 °C for 20 s, 60 °C for 20 s, and 72 °C for 1 min (20 cycles). The amplicons of the first two reactions were combined in equimolar amounts, denatured at 95 °C for 20 s, extended and enriched by another 25 cycles of amplification with cDNA-NAM or cDNA-SAU and cDNA-2A using TaKaRa Ex Taq™ (Takara). The resulting *ca.* 2.2 kb DNA fragment (containing either pNAM/SAT or pSAU/SAT mutations) was digested with SspI and XmaI and cloned into the corresponding region of pSAT2. The mutations were verified by nucleotide sequencing of the complete P1-coding region using selected oligonucleotides and no unintended site mutations were found.

2.4. *In vitro* RNA synthesis, transfection and virus recovery

Plasmids containing genome-length cDNAs, chimeric cDNA or site-directed mutated cDNA clones were linearised at the SwaI site downstream of the poly-A tract and used as templates for RNA synthesis utilising the MEGAscript™ T7 kit (Ambion). Transcript RNAs were examined in agarose gels for their integrity and quantitated by spectrometry. BHK-21 cell monolayers in 35 mm cell culture plates (Nunc™) were transfected with 2–3 μg of the *in vitro* synthesised RNA using Lipofectamine2000™ (InVitrogen). Transfected monolayers were incubated at 37 °C with a 5% CO_2 influx for 48 h in Eagle's basal medium (BME) containing 1% foetal calf serum (v/v) and 25 mM HEPES. The virus-containing supernatants were used to infect fresh BHK-21 monolayers (35 mm cell culture plates) using 1/10th of clarified infected supernatants and incubated for 48 h at 37 °C. Viruses were subsequently harvested from infected cells by a freeze–thaw cycle and passaged four times on BHK-21 cells, using 10% of the supernatant of the previous passage. Following the recovery of viable viruses, the presence of the mutations was verified once again with automated sequencing.

2.5. *Evaluation of the ability of SAT types of FMDV to infect and replicate in CHO-K1 cells*

Twenty-four hours growth kinetics was performed in CHO-K1 cells which express GAG receptors (Jackson et al., 1996; Sa-Carvalho et al., 1997). Monolayers of CHO-K1 cells in 35 mm cell culture plates were infected with a MOI of 5–10 of the parental and vaccine strains (Table 1) for 1 h or 24 h at 37 °C. Infected monolayers were then frozen at −70 °C and thawed. Viruses from the lysed monolayers were titrated on BHK-21 monolayers and viral growth was calculated by subtracting the 24 h titre results from the 1 h titre results. Positive titers were an indication that the viruses are able to infect and replicate in CHO-K1 cells, suggesting the ability to utilise GAG receptors for cell entry. The nucleotide sequences of the isolates that were able to infect and replicate in CHO-K1 cells within 24 h were determined and compared to those of the parental viruses.

2.6. *Sequence alignments and structural modelling*

Homology models of the capsid proteins (VP1-4) for a representative virus of each of the SAT1 and two serotypes (SAT1/SAR/9/81, SAT2/ZIM/7/83) were built using Modeller 9v3 (Sali and Blundell, 1993) with 1FOD (Logan et al., 1993) as the template. SAR/9/81 and ZIM/7/83 capsid proteins were aligned with that of O1BFS

Table 2
Comparison of the capsid amino acid sequences of the SAT1 and SAT2 primary isolates and their cell culture-adapted derivatives.

Protein	β–β Structure	SAT1 isolate[a]			
		SAR/9/81	KNP/196/91	NAM/307/98	ZAM/2/93
VP2	βB-βC	–	Q2074R[b]	–	–
		–	Q2170H	–	–
		–	S2196N	–	–
VP3		–	D3009V	–	–
	βE–βF	–	–	**E3135K**[b]	–
	βG–βH	–	–	**E3175K**[b]	–
		–	–	–	A3180V
		D3192Y	–	–	–
		–	–	S3203T	–
		S3217I	–	–	–
		–	–	S3219L	–
VP1		–	Y1018H	–	–
		–	–	T1025A	–
		–	–	A1033T	–
		–	R1049K	–	–
		A1069G	–	–	–
		–	–	–	K1086Q
	βF–βG	**N1110K**[b]	**K1110K**[b]	–	–
	βF–βG	–	–	–	**N1111K**[b]
		G1112R[b]	**G1112R**[b]	G1112D	**G1112R**[b]
		–	–	K1157A	–
		–	–	E1177Q	–
		–	V1179E	–	–
		–	K1206R	–	–
		–	K1210R	–	–

Protein	β–β Structure	SAT2 isolate[a]			
		KNP/19/89	ZIM/5/83 vs. ZIM/7/83	ZAM/7/96	ZIM/14/90
VP2		I2032V	–	–	–
		–	M2077T	–	–
		–	–	–	E2096Q
	βG–βH	–	–	–	**Q2170R**[b]
VP3		H3036	–	–	–
		T3043S	–	–	–
		Q3049E	–	–	–
	βE–βF	–	–	–	**T3129K**[b]
		–	–	–	D3132N
		–	–	E3148K	–
		P3192T	–	–	–
VP1		–	M1028V	–	–
		–	A1064G	–	–
	βD–βE	–	–	**E1083K**[b]	–
	βD–βE	**Q1085R**[b]	–	–	–
		R1098T	–	–	–
	βG–βH	–	**E1161K**[b]	–	–
		–	Y1169H	–	–
		T1171A	–	–	–
		F1194L	–	–	–
		V1207A	–	–	–

[a] The amino acid residues have been numbered independently for each protein. For each residue, the first digit indicates the protein (VP1, VP2 or VP3) and the last three digits the amino acid position in either a SAT1 or SAT2 alignment. The P1 polypeptide of SAT1 viruses is 744 amino acids and that of SAT2 viruses 741 amino acids.
[b] Amino acid changes to a positive charge in surface-exposed loops are shown in bold.

using ClustalX and the sequence similarities for both were above 80%. The homology structure was calculated by the satisfaction of spatial restraints as described by empirical databases. Structural checks of the model were done using WHAT CHECK (Hooft et al., 1996).

The complete P1 sequences of 56 low passage SAT viruses (26 SAT1 and 30 SAT2) from 17 different countries in Africa, available on GenBank, were translated in BioEdit and aligned using ClustalX. The viruses used in the alignment were isolated from clinical material on PK cells and grown 1–4 passages in IBRS-2 cells (Bastos et al., 2001, 2003) and were referred to as wild-type viruses. The P1 sequences of the wild-type viruses were compared to the BHK-21 adapted viruses.

3. Results

3.1. Adaptation of SAT viruses in cell culture selects variants that gain a net positive charge on the virion surface

SAT viruses used for vaccine production are typically adapted to cultured cells following limited passages in BHK-21 cells. In this study, we have investigated the phenotypic and genetic changes associated with the transition of SAT viruses from wild-type to the cell culture-adapted phenotype. The morphology of virus plaques produced on BHK-21 cell monolayers following infection with SAT1 and SAT2 vaccine strains differed from the plaques produced by the parental strains which have not been adapted to BHK-21 cell

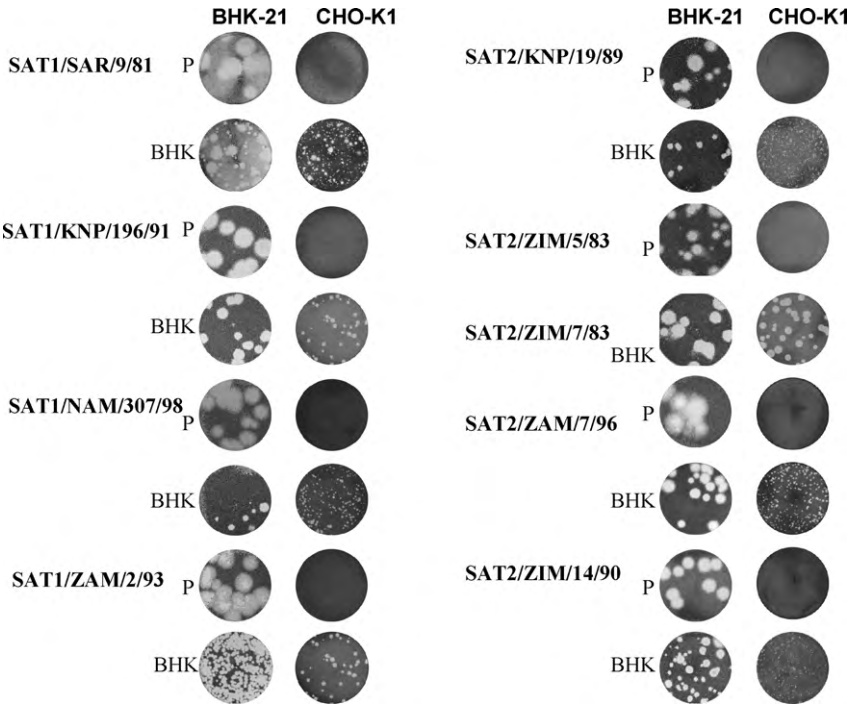

Fig. 1. Plaque morphologies of the parental (P) and cell culture (BHK) derived viruses obtained using monolayers of BHK-21 and CHO-K1 cells. Cells infected with the indicated viral strains were incubated with tragacanth overlay for 40 h prior to staining with 1% methylene blue. Plaques for SAT1 and SAT2 wild-type viruses are generally large with opaque edges and adaptation is accompanied by smaller to medium plaques and clear edges.

culture (Fig. 1). In particular, SAT1/KNP196/91^{P} (isolated on primary pig kidney cells) and SAT1/SAR/9/81^{P} (epithelium of infected impala) viruses displayed large plaques (7–8 mm) with opaque edges. In contrast, plaques produced by the corresponding vaccine derivatives, KNP/196/91^{Vac} and SAR/9/81^{Vac} viruses (high passage), exhibited a mixture of small (1–2 mm), medium (3–4 mm) to large plaques with clearly defined edges. Whereas the parental strains failed to infect CHO-K1 cells, both vaccine strains produced small and clear plaques on CHO-K1 cells (Fig. 1) and reached titers of 2.8×10^6 and 1.1×10^6 pfu/ml after 24 h growth on CHO-K1 cells, respectively (Table 1). Table 2 summarizes the amino acid differences of the low and high passage viruses. Comparison of the amino acid sequence in the outer capsid proteins of the KNP196/91^{P} and KNP/196/91^{Vac}, in particular, revealed 11 amino acid substitutions in the adapted strain, *i.e.* three substitutions in VP2, one in VP3 and seven in VP1.

The structural location of these 11 residues in the capsid proteins was mapped to a SAT1 capsid protomer. Fig. 2 illustrates two substitutions, the first in VP1 (Gly112 → Arg) and the second in VP2 (Gln74 → Arg), of neutral amino acids with positively charged residues which are located within surface-exposed loops that connect β-sheet structures. The Gln74 → Arg substitution in VP2 is located in the βB–βC loop which is characteristically hypervariable (see Table 3 for details). The proximity of this substitution to three other positively charged residues, Lys206 → Arg, Arg208 and Lys210 → Arg, located in the C-terminus of VP1 (Table 2 and Fig. 2) is noteworthy since these residues were reported to form part of the walls of a heparin-binding depression of serotype A viruses (Fry et al., 2005). Positively charged residues were found to be conserved at these positions in a complete alignment of SAT1 isolates (data not shown). The Gly112 → Arg substitution in VP1 forms part of a novel sequence in the βF–βG loop comprising three residues (KGG for KNP/196/91^{P}) where positively charged residues (KGR) accumulated during cell culture adaptation of SAT1 viruses (Table 2). The altered amino acid sequence correlates with the Asn110 → Lys and Gly112 → Arg substitutions in the VP1 protein of SAT1/SAR/9/81^{Vac}. The 3D structural model of a protomeric unit revealed that the positively charged SAT1 substitutions, at positions 110 and 112 in each of the interacting VP1 subunits, surround the pore located at the fivefold axis of the virion (Fig. 2). An interesting observation was that adjacent to this positively charged sequence of the VP1 βF–βG loop a Val was selected for in the place of an Asp at position 9 of VP3 in KNP/196/91^{Vac} (Table 2; Fig. 2) which may increase the local positive charge on the virion surface even more and increase the virus' ability to adhere to negatively charged sulfated polysaccharides.

Similar to KNP/196/91 and SAR/9/81, two other SAT1 field viruses (NAM/307/98 and ZAM/2/93) adapted and acquired the ability to infect CHO-K1 cells upon repeated passages in BHK-21 cells. The parental NAM/307/98 virus, isolated from buffalo (*Syncerus caffer*) in the West Caprivi Game Reserve in Namibia in 1998 (Bastos et al., 2001; Storey et al., 2007) underwent slow adaptation to cell culture, only attaining titers of 10^5 pfu/ml after eight passages in BHK-21 cells, and progeny viruses failed to infect CHO-K1 cells (Fig. 1). Only following repeated passaging in BHK-21 cells, this isolate finally adapted to BHK-21 cells (NAM/307/98^{BHK}) as measured by its ability to infect CHO-K1 cells and by producing titers in excess of 10^7 pfu/ml in BHK-21 cells (Table 1). NAM/307/98^{BHK} yielded clear plaques of small (1–2 mm) and medium (3–5 mm) sizes and acquired the ability to infect CHO-K1 cells (Fig. 1). Sequence analysis revealed nine amino acid substitutions in the capsid proteins of the adapted strain (Table 2). Only two of these were positively charged and located within surface-exposed loops of VP3, *i.e.* residues Glu135 → Lys and Glu175 → Lys. The residues are located around the threefold axis of the pentamer unit (Fig. 2). Another SAT1 field isolate, ZAM/2/93 (Fig. 1), adapted rapidly in BHK-21 cells, only requiring two rounds of passaging, and the progeny viruses acquired two positively charged amino acids at position 111–112 of VP1 (Asn111 → Lys and Gly112 → Arg) (Table 2). This result is in agreement with the substitutions observed for the SAT1 vaccine strains KNP/196/91 and SAR/9/81. Therefore, we have identified a sequence "hotspot"

Table 3
A summary of the amino acid variation in the putative HSPG-binding sites identified for SAT1 and SAT2 BHK-21 adapted strains. The residue variation was obtained from complete P1 alignments of 24 SAT1 and 24 SAT2 field viruses.

	Amino acid variation					
	VP2	VP3		VP1		
	2074[a]	3135	3175	1083–1085	1110–1112	1161
SAT1	Q/R/A/K/E/N/S	E/N/A/D/V/S/T	E		N/K/H/R/A/T-G/N/D-G/N/D	
SAT2				E/D/I/T/K-H-E/R/K/T/S/Q/A		T/A/E/S/Q

/ denotes differences at the same aa position and "-" indicates the next aa.
[a] The first digit indicates the protein (VP1, VP2 or VP3) and the last three digits the amino acid position in either a SAT1 or SAT2 alignment.

(amino acids 110–112 of VP1) for the accumulation of positive charges during cell culture adaptation of SAT1 viruses.

We subsequently investigated whether SAT2 viruses that have acquired BHK-21 cell adaptation, do so by selecting positive charge substitutions in "hotspots" on the external capsid proteins. The SAT2 vaccine strain KNP/19/89^{Vac} (Table 1) was originally isolated from buffalo in the Kruger National Park (KNP/19/89^{P}). Whereas the viral plaques produced by the KNP/19/89^{Vac} strain on BHK-21 monolayers were medium (3–5 mm) in size and clearly defined, those produced on CHO-K1 cells were needle point (<1 mm) to small (1–2 mm) in size (Fig. 1). The KNP/19/89^{Vac} attained a titer of 5×10^6 pfu/ml at 24 h post-infection of CHO-K1 cells (Table 1). Another SAT2 vaccine strain, ZIM/7/83, passaged five times in BHK-21 cells, infected and replicated effectively in CHO-K1 cells, reaching a titer of 6.5×10^6 pfu/ml 24 h post-infection of CHO-K1 cells (Table 1), and produced medium-sized plaques in this cell line. The parental virus ZIM/5/83 failed to grow in CHO-K1 cells. For the two SAT2 vaccine strains (KNP/19/89^{Vac} and ZIM/7/83), only substitutions in VP1, *i.e.* Gln85 → Arg for KNP/19/89 and Glu161 → Lys for ZIM/7/83 (Table 2), effected in significant charge difference on the virion surface (Fig. 2). The latter substitution in VP1 is preceded by two positively charged residues, *i.e.* Lys159–His160, at the C-terminal base of the βG–βH loop. The Gln85 → Arg found in KNP/19/89^{Vac}, is structurally neighbouring the fivefold axis of the virion and forms part of a three positively charged amino acid sequence in the βD–βE loop of VP1. However, since VP1 residue 85 was conserved as Glu in ZIM/7/83, the amino acids at position 159–161 (Lys–His–Glu) of VP1 that changed to Lys–His–Lys in the vaccine strain may be necessary for BHK-21 cell adaptation in this strain.

The role of the three residues at position 83–85 in VP1 in the cell culture adaptation of SAT2 viruses was supported following the adaptation and characterisation of the field virus ZAM/7/96 (Table 1), isolated from buffalo (Bastos et al., 2003). Whereas this parental isolate produced large (6–7 mm) plaques on BHK-21 monolayers, the cell culture-adapted variant produced a mixture of medium (3–5 mm) and large plaques and was able to infect CHO-K1 cells, unlike its parental counterpart (Fig. 1). A Glu → Lys substitution was observed at position 83 of VP1, as well as residue 148 of VP3 (Table 2). Whether the two substitutions contributed synergistically or independently to the cell culture-adapted phenotype is not known. The ability of high passage ZIM/14/90 to infect and replicate in CHO-K1 cells (Fig. 1) was associated with Gln170 → Arg and Thr129 → Lys substitutions in VP2 and VP3,

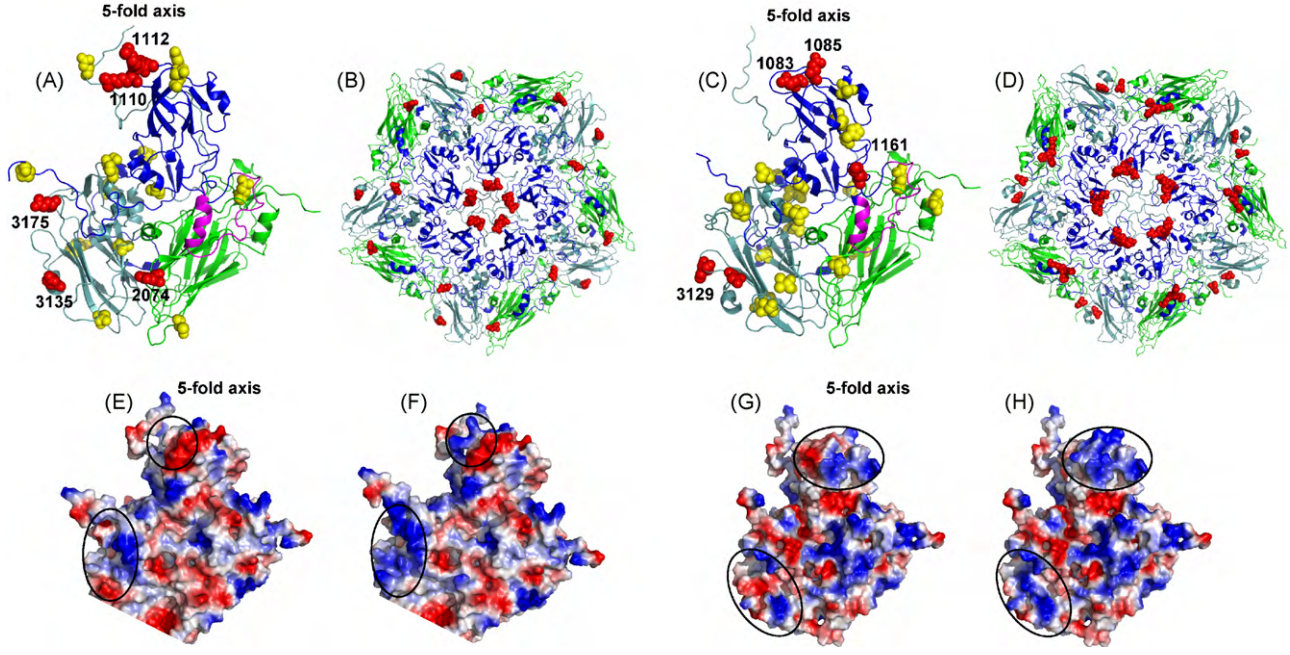

Fig. 2. 3D structure of a SAT1 and SAT2 protomeric subunit (A and C) and pentamer (B and D), modelled using the O1BFS co-ordinates (1FOD) as template. (A and B) The position of surface-exposed positive charge amino acid changes observed in cell culture-adapted SAT1 viruses is indicated in red. KRR, KGR and HRK positively charged residues were observed for SAR/9/81, KNP/196/91 and ZAM/2/93 at residue positions 110–112 of VP1. Lysines were present at residues 135 and 175 of VP3 in NAM/307/98 and an arginine at position 74 of VP2 in KNP/196/91. (C and D) For SAT2 viruses the positively charged residues at VP1 positions 83 and 85 (red) is surrounding the pore at the fivefold axis. The protein subunits and structural features for both models are colour coded: VP1 (blue), VP2 (green) and VP3 (light-teal), the G–H loop of VP1 containing the RGD motif (magenta). Other residue changes observed in SAT1 and SAT2 viruses are shown in yellow (see Table 2 for detail). (E–H) The electrostatic, accessible surface view of the SAT1 and SAT2 modelled biological protomers are shown. The electrostatic potential was coloured with positive charge as blue and negative in red and the scale of colouring was kept constant. The position of the charge change during adaptation is outline in black and is shown from E to F for SAT1 and G to H for SAT2 viruses.

respectively (Table 2). As indicated in Fig. 2, the selection of positively charged residues during adaptation occurred against a background of existing positive charges on the virion surface.

3.2. Genetic characterisation of residues involved in binding to CHO-K1 cells

Examination of the outer capsid protein sequences of 26 SAT1 and 30 SAT2 viruses from our database revealed a high level of variability at the residue positions associated with change during cell culture adaptation of the viruses (Table 3). For instance, residue 74 of VP2 is characterised by high entropy (Hx > 1.5) and forms part of a variable loop extending from residue 60–85, as is evident from a complete alignment of the capsid proteins of SAT1 viruses. At least 30% of the SAT1 viruses ($n = 8$) in the complete capsid protein alignment contained a Lys or Arg residue at position 74. However, the SAT1 isolates ($n = 26$) did not display the ability to infect and replicate in CHO-K1 cells (results not shown). In contrast, residue position 135 of VP3, also characterised by high entropy (Hx > 1.8), does not contain positively charged residues in any of the SAT1 field isolates, while position 175 of VP3 contains a conserved Glu residue in all 26 isolates. The VP1 residues 110–112, located in the short, variable βF–βG loop, display entropy of Hx > 0.7 and the absence of positively charged amino acids at positions 111 and 112. Where a Lys or Arg residue did occur at position 110, it was, however, followed by a negatively charged Asp residue at positions 111 or 112 in 50% of the cases.

A complete amino acid alignment of 30 SAT2 field isolates depicted the βD–βE loop of VP1 as a hypervariable region with residues 83 and 85 displaying high entropy (Hx > 1.3), while the His at position 84 was conserved. Only one isolate, KEN/3/57, an archive vaccine strain, contained a Lys–His–Lys sequence at this position, similar to that observed in a vaccine strain, KNP/19/89^{Vac}, and an adapted strain, ZAM/7/96^{BHK}. An Arg residue was repeatedly observed at position 85 of VP1 during adaptation of KNP/19/89 to BHK-21 cells. Residue 161 of VP1 was found to be variable in SAT2 viruses and a Lys residue was present at this position only in the cell culture-adapted strain ZIM/7/83^{Vac}. Notably, this residue follows two other positively charged residues, Lys159–His160, in VP1 of this virus.

The genetic changes observed in the case of cell culture-adapted SAT2/ZIM/14/90 were more complex and their implication for cell adaptation was less apparent (Table 2). From a structural perspective, the acquired positively charged residues at position 170 of VP2 and 129 of VP3 were neither surface exposed, nor were they located in the small heparin-binding depression (Fry et al., 2005) on the virion surface (Fig. 2). These changes were selected against a background of existing positively charged residues surrounding the threefold axis of the virus. This resulted in an increase in the positive polarity at local regions of the virion. In support of this observation was the finding that selection occurred against a negatively charged Asp residue at position 132 of VP3, which mutated to an Asn. Residues 129 and 132 of VP3 are located within a highly variable region, as observed from the P1 alignment of 30 SAT2 viruses, and the possibility that this area may function as an epitope cannot be excluded.

3.3. Generation and characterisation of recombinant viruses with altered surface charges

To study the effect of individual mutations in a defined genetic background, we constructed recombinant virus mutants in FMDV SAT2 infectious cDNA. Of the 26 SAT1 and 21 SAT2 amino acid changes introduced during cell culture adaptation of the parental virus isolates, we selected the following residue positions in VP1 for the generation of site-directed mutant recombinant viruses (Fig. 3A): (1) RGD to KRR at position 110–112 in a SAT1/SAT2 chimeric construct, *i.e.* pNAM/SAT (Storey et al., 2007); (2) Gln85 → Arg which increased the net positive charge of VP1 surrounding the fivefold axis of SAT2 virions and (3) Glu161 → Lys which was unique in that SAT2/ZIM/7/83 accumulated three positively charged residues at the base of the βG–βH loop. The latter two mutations were constructed in a SAT2/SAT2 chimeric infectious clone, pSAU/SAT, containing the outer capsid-coding region of the SAT2/SAU/6/00 virus in the pSAT2 genetic background (Böhmer, 2004). The SAU/6/00 isolate caused a severe outbreak in dairy herds in Saudi Arabia in 2000. However, production of a SAU/6/00 vaccine is hindered by low 146S antigen yields, a consequence of SAU/6/00 being notoriously difficult to adapt to BHK-21 cells.

The effect of these mutations on surface charge distributions is shown in Fig. 2(E, F and G, H). The SAT1 mutations at position 110–112 (Fig. 2E and F) and the SAT2 mutations at position 83–85 of VP1 (Fig. 2G and H) had a strong effect on the local surface electrostatic potential. A distinct local surface area, neighbouring the fivefold axes, lost its negative charge and gained a predominantly positive charge in both SAT1 and SAT2 viruses, although the amino acid positions were dissimilar. However, the positively charged region spanning residues 159–161 of the SAT2 vaccine strain (ZIM/7/83), was located at the base of the βG–βH loop and did not conform to the region surrounding the fivefold axis or the depression at the VP2/VP3/VP1 border (Fry et al., 2005).

Viable recombinant mutant viruses, designated vNAM(KRR)/SAT, vSAU(E85R)/SAT and vSAU(E161K)/SAT, were recovered from all three mutant clones and passaged in BHK-21 cells until CPE was observed (3–5 passages). Sequencing of the capsid-coding region of the progeny viruses revealed that the introduced KRR mutation was fixed in the population as a KGR sequence, but no other unintentional mutations were introduced in the mutant viruses.

3.4. Plaque phenotypes and relative infectivity titers

We subsequently investigated the ability of the recombinant mutant viruses to infect CHO-K1 cells, and the effect these mutations had on infectivity titers in BHK-21 cells. Confirmation of the role of positively charged residues, located at position 110–112 in VP1 of SAT1 vaccine strains, in the adaptation to BHK-21 cells was obtained by introducing a KRR sequence into the vNAM/SAT interserotype chimeric virus. The vNAM/SAT virus contain the outer capsid-coding region of a Namibian buffalo isolate, *i.e.* NAM/307/98 (Bastos et al., 2001), and displays poor growth and adaptation to BHK-21 cells. Furthermore, vNAM/SAT lacked BHK-21 cell culture adaptation as measured by the inability to infect CHO-K1 cells and poor titers on BHK-21 cells. The plaques in Fig. 3B illustrate the transition of the large, opaque wild-type plaques produced by the vNAM/SAT (wild-type outer capsid) to small, well-defined plaques on BHK-21 cell monolayers of the mutated progeny virus, vNAM(KRR)/SAT. The vNAM(KRR)/SAT also attained titers of 10^6 pfu/ml within 5 passages in BHK-21 cells, while viruses harbouring the corresponding wild-type outer capsid-coding region only produced titers of 10^5 pfu/ml after eight passages. In summary, the mutations in the VP1 βF–βG loop neighbouring the fivefold axis of the SAT1 viruses, a site prone to variation, conferred the ability to adapt rapidly to BHK-21 cells and grow in CHO-K1 cells. This ability of the virus is probably due to utilisation of alternative HSPG receptors for cell binding and entry in cultured cells.

The effect of an Arg at VP1 position 83 or a Lys at 161 of vSAU/SAT is shown in Fig. 3B. No significant differences were observed in the plaque morphologies of the progeny virus populations obtained from the non-mutated vSAU/SAT and vSAU(E85R)/SAT and vSAU(E161K)/SAT mutated viruses (Fig. 3B). On BHK-21 mono-

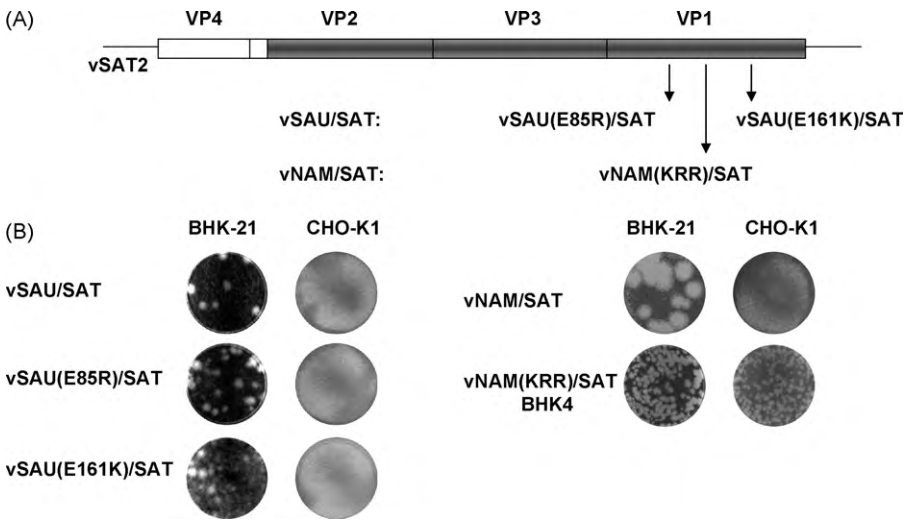

Fig. 3. (A) Schematic representation of the chimeric FMDV constructs and the introduction of mutations described in this study. (B) Plaque morphologies of chimeric viruses containing the wild-type outer capsid proteins of SAT1/NAM/307/98 and SAT2/SAU/6//00 cloned into the genetic background of pSAT2. The change in plaque phenotype on BHK-21 cells and the susceptibility of CHO-K1 cells for infection by the mutant vNAM(KRR)/SAT is shown. The mutant vSAU(E85R)/SAT and vSAU(E161K)/SAT displayed the same plaque morphology than the wild-type chimera and did not grow in CHO-K1 cells.

layers, the virus plaques were opaque, a phenotype commonly associated with viruses which have not been adapted to BHK-21 cells. Furthermore, CHO-K1 cells were not able to sustain infection by the vSAU/SAT or mutated virus populations. The infectivity titers on BHK-21 cells were also comparable for the three virus populations. Neither vSAU/SAT, nor the two mutants, vSAU(E85R)/SAT and vSAU(E161K)/SAT, were able to utilise HSPG for cell entry.

An in-depth analysis of the amino acid sequences neighbouring the introduced mutations in vSAU/SAT revealed that the introduced Lys85 was preceded by an acidic Glu residue at position 83, while the Lys161 was preceded by a DSTH sequence at VP1 residue positions 157–160. In both instances the added positive charge was compromised by acidic residues in its immediate environment, which may explain the absence of interaction with the negatively charged HSPG molecules.

4. Discussion

Despite the success of conventional vaccines in the control of FMD in the developed world, inactivated vaccines are unable to cover the vast antigenic variability within the SAT types in southern Africa (Hunter, 1996). Recombinant inactivated SAT type vaccines, structurally designed to be effective for specific geographic regions, may overcome the limitation of antigenic variation (Van Rensburg et al., 2004). However, the transfer of antigenic determinants during the replacement of the outer capsid proteins is simultaneously accompanied by the transfer of the receptor preferences of the field isolate. This could impact adversely on the use of recombinant viruses as vaccine seed stock due to the lack of cell culture adaptation and the consequent low yields in 146S particles. In addition, adaptation to the BHK-21 production cell line is often a cumbersome, time consuming and expensive process (Rieder et al., 1993; Van Rensburg et al., 2004).

To address the limitation of acquiring this adaptation phenotype by selection, we investigated the accumulated genetic changes of SAT1 and SAT2 viruses which have been adapted to BHK-21 cells, including efficacious vaccine strains. Our study supports the evidence from diverse virus families that cell culture adaptation of viruses (Patel et al., 1993; Chen et al., 1997; Krusat and Streckert, 1997; Byrnes and Griffin, 1998; Klimstra et al., 1998; Summerford and Samulski, 1998), and more specifically, FMDV (Jackson et al., 1996; Sa-Carvalho et al., 1997; Fry et al., 1999), selects from the quasi-species population variants with affinity for HSPG as observed by the ability to infect and replicate in CHO-K1 cells. Comparison of the outer capsid proteins of SAT1 and SAT2 viruses, with and without this phenotype, revealed a pattern of mutations with the common property of increasing the net positive charges on the virion surface, particularly surrounding the fivefold axis of the virion. Adaptation of the viruses in BHK-21 monolayer cells select for positively charged, surface-exposed residues which are most probably involved in the facilitation of cell entry via HSPG molecules.

Binding of viruses to HSPG or other GAGs occurs mainly through electrostatic interactions between positively charged Lys and Arg groups on the virus surface and the negatively charged N and O sulfated groups of the GAG molecules (Gromm et al., 1995; Byrnes and Griffin, 1998, 2000). Similarly to FMDV, repeated passaging of alphaviruses in BHK-21 cells also leads to reduced plaque size and an increased HSPG-binding ability (Marshall et al., 1962; Heydrick et al., 1966; Byrnes and Griffin, 1998). The accumulated positively charged residues and increased affinity to HSPG probably leads to direct interaction between the Arg or Lys and the polysaccharide backbone. In numerous other HSPG-binding proteins the strength of binding to the substrate was affected by the degree of sulfation of the polysaccharide backbone (Byrnes and Griffin, 1998). The selection of positively charged residues during cell-culture adaptation was previously reported for type O viruses (Sa-Carvalho et al., 1997; Jackson et al., 1996, 2001). Adaptation of the O1 Campos virus to cell culture selected viruses with an H → R change at position 56 of VP3 (Jackson et al., 1996; Sa-Carvalho et al., 1997). The 3D structure of the virion revealed that the positively charged residue 56 of VP3 is located within the recessed heparin-binding site, a depression on the virion surface situated at the junction of VP1, VP2 and VP3 (Fry et al., 1999).

Although we did not observe any of these changes in the VP3 proteins of the SAT1 or SAT2 viruses, residue changes at positions 135 and 175 in the VP3 were present in SAT1/NAM/307/98. Both these changes may contribute singly or accumulatively to the adaptation phenotype. The effect of each of these changes individually and accumulatively on cell culture adaptation and possible HSPG-binding is, therefore, not known and needs investigation to fully understand the mechanisms of cell culture adaptation. Furthermore, this is the first report on the fixation of positively charged residues 110–112 in the βF–βG loop of VP1 of SAT1 isolates and

its possible correlation with the ability of SAT1 viruses to replicate in CHO-K1 cells. The importance of this amino acid sequence in adaptation of SAT1 isolates to cultured BHK-21 cells and its possible function as a HSPG-binding site is evident from: (1) the KNP/196/91^{Vac} and SAR/9/81^{Vac} vaccine strains (Fig. 1) with the ability to infect and replicate in CHO-K1 cells; (2) the field isolate ZAM/2/93 adapted rapidly to cell culture as observed by the appearance of small plaques on BHK-21 cells and growth in CHO-K1 cells; (3) variation at the residue positions 110 and 112 of the VP1 capsid protein in an alignment of 26 SAT1 wild-type viruses with the inability to grow on CHO-K1 cells (Table 3); and (4) the introduction of the positively charged residues 110–112 in the vNAM/SAT chimeric virus was consistent with the small plaque phenotype and growth in CHO-K1 cells of the KNP/196/91 and SAR/9/81 vaccine strains. With the exception of SAT1/KNP/196/91, none of the other SAT1 viruses showed genetic changes in VP2 between the primary isolates and cell culture-adapted derivatives. The Gln74 → Arg substitution in VP2 is structurally associated with the shallow depression observed at the junction of the three major capsid proteins described by Fry et al. (2005).

The only mutations in VP3 observed during adaptation of SAT2 viruses were the Glu148 → Lys change of ZAM/7/96 and the Thr129 → Lys substitution of ZIM/14/90, although both residues were not fully exposed on the virion surface and did not correlate with the shallow HSPG-binding depression (Fry et al., 2005). These mutations, however, did not occur in isolation in these viruses and were possibly selected against a background of existing positively charged residues (Fig. 2). In the case of Thr129 → Lys mutation, it was accompanied by an Asp132 → Asn mutation, with the removal of a surface-exposed negative charge. Whether the two substitutions contributed synergistically or independently to the cell culture adaptation phenotype is not known. The ability of ZIM/14/90 to infect and replicate in CHO-K1 cells (Fig. 1) was associated with Gln170 → Arg change in VP2 together with the Thr129 → Lys substitution in VP3, an indication that the accumulative contribution may play a role. Noteworthy is the observation of existing positively charged residues in close approximation of these changes, suggesting that the selection of positively charged residues during adaptation transpired against a background of existing positive charges on the virion surface. The residue changes at position 83–85 of VP1 were observed for both the SAT2 viruses, KNP/19/89 and ZAM/7/96. The role of these residues, protruding from the fivefold axis, in BHK-21 adaptation and possible binding of HSPG is in agreement with observation for SAT1 viruses.

Phenotypic characterisation of the recombinant mutants revealed that the variants that were able to infect CHO-K1 cells shared a small plaque phenotype in BHK-21 cells. The small plaque phenotype produced by the vNAM(KRR)/SAT mutant in BHK-21 cells was consistent with the small plaques observed for the SAT1 vaccine strains SAR/9/81^{Vac} and KNP/196/91^{Vac}. Introduction of the cell culture adaptation phenotype during the construction of a chimeric virus may thus be advantagous for improved infectivity in cultured BHK-21 cells used in the production of FMD vaccines. On the contrary, neither vSAU(E85R)/SAT nor vSAU(E161K)/SAT produced plaques with altered morphology on BHK-21 cells compared to vSAU/SAT with the wild-type outer capsid. A systematic analysis of the sequences adjacent to both mutations revealed the presence of negatively charged residues which may act as a repelling force to the negatively charged sulfated groups of GAG's. Therefore, the role of the VP1 amino acid sequences of SAT2 isolates in cell culture adaptation requires further investigation.

The development of new vaccine strains to protect against emerging SAT viruses relies strongly on the virus yield of the new strain in the production cell line, the yield of 146S particles, stability of the virus and antigen, and a close antigenic relationship to field isolates causing current FMD outbreaks. BHK-21 cells are the cell line of choice for production of inactivated FMD vaccines and SAT viruses are notorious for their difficulty to adapt to BHK-21 cells (as outlined in Section 1). Our results demonstrated that for the purpose of SAT type vaccine production, viruses previously impossible to adapt to cell culture, can be designed with improved growth properties in cell cultures. Introductions of the cell culture adaptation phenotype to chimeric FMDV may be beneficial to the productivity in BHK-21 cells and the production 146S antigen.

Acknowledgments

This work was supported by funding from Intervet–Schering-Plough and the U.S. Department of Agriculture, Agricultural Research Service. The cell culture-adapted SAT1 and SAT2 viruses were received from the vaccine unit at Transboundary Animal Diseases of the ARC-OVI. We thank Juanita van Heerden for her contributions with sequencing part of SAT2/KNP/19/89. We would also like to thank Dr. Otto Koekemoer, Ms. Sonja Maree and Erika Kirkbride for critical reading of the manuscript.

References

Acharya, R., Fry, E., Stuart, D., Fox, G., Rowlands, D., Brown, F., 1989. The three-dimensional structure of foot-and-mouth disease virus at 2.9 Å resolution. Nature 337, 709–716.

Almeida, M.R., Rieder, E., Chinsangaram, J., Ward, G., Beard, C., Grubman, M.J., Mason, P.W., 1998. Construction and evaluation of an attenuated vaccine for foot-and-mouth disease, difficulty adapting the leader proteinase-deleted strategy to the serotype O1 virus. Virus Res. 55, 49–60.

Amadori, M., Berneri, C., Archetti, I.L., 1994. Immunogenicity of foot-and-mouth disease virus grown in BHK-21 suspension cells. Correlation with cell ploidy alterations and abnormal expression of the alpha 5 beta 1 integrin. Vaccine 12, 159–166.

Amadori, M., Volpe, G., Defilippi, P., Berneri, C., 1997. Phenotypic features of BHK-21 cells used for production of foot-and- mouth disease vaccine. Biologicals 25, 65–73.

Bastos, A.D.S., 1998. Detection and characterization of foot-and-mouth disease virus in sub-Saharan Africa. Onderstepoort J. Vet. Res. 65, 37–47.

Bastos, A.D.S., Haydon, D.T., Forsberg, R., Knowles, N.J., Anderson, E.C., Nel, L.H., Thomson, G.R., Bengis, R.G., 2001. Genetic heterogeneity of SAT-1 type foot-an-d-mouth disease viruses in southern Africa. Arch. Virol. 146, 1537–1551.

Bastos, A.D.S., Haydon, D.T., Sangare, O., Boshoff, C.I., Edrich, J.L., Thomson, G.R., 2003. The implications of virus diversity within the SAT 2 serotype for control of foot-and-mouth disease in sub-Saharan Africa. J. Gen. Virol. 84, 1595–1606.

Baxt, B., Becker, Y., 1990. The effect of peptides containing the arginine–glycine–aspartic acid sequence on the adsorption of foot-and-mouth disease virus to tissue culture cells. Virus Genes 4, 73–83.

Berinstein, A., Roivainen, M., Hovi, T., Mason, P.W., Baxt, B., 1995. Antibodies to the victronectin receptor (Integrin $\alpha_v\beta3$) inhibit binding and infection of foot-and-mouth disease virus to cultured cells. J. Virol. 69, 2664–2666.

Böhmer, B., 2004. Engineering of a chimeric SAT2 foot-and-mouth disease virus for vaccine production. M.Sc. thesis, University of Pretoria, South Africa.

Byrnes, A.P., Griffin, D.E., 1998. Binding of Sindbis virus to cell surface heparan sulfate. J. Virol. 72 (9), 7349–7356.

Byrnes, A.P., Griffin, D.E., 2000. Large-plaque mutants of Sindbis virus show reduced binding to heparan sulfate, heightened viremia, and slower clearance from the circulation. J. Virol. 74, 644–651.

Chen, Y., Maguire, T., Hileman, R.E., Fromm, J.R., Esko, J.D., Linhardt, R.J., Marks, R.M., 1997. Dengue virus infectivity depends on envelope protein binding to target cell heparan sulfate. Nat. Med. 3, 866–871.

Cottam, E.M., Thébaud, G., Wadsworth, J., Gloster, J., Mansley, L., Paton, D.J., King, D.P., Haydon, D.T., 2008. Integrating genetic and epidemiological data to determine transmission pathways of foot and mouth disease virus. Proc. Biol. Sci. 275 (1637), 887–895.

Curry, S., Fry, E., Blakemore, W., Abu-Ghazaleh, R., Jackson, T., King, A., Lea, S., Newman, J., Stuart, D., 1997. Dissecting the roles of VP0 cleavage and RNA packaging in picornavirus capsid stabilization, the structure of empty capsids of foot-and-mouth disease virus. J. Virol. 71, 9743–9752.

Duque, H., Baxt, B., 2003. FMDV receptors: comparison of bovine av integrin utilization by type A and O viruses. J. Virol. 77, 2500–2511.

Fox, G., Parry, N.R., Barnett, P.V., McGinn, B., Rowlands, D.J., Brown, F., 1989. The cell attachment site on foot-and-mouth disease virus includes the amino acid sequence RGD (arginine–glycine–aspartic acid). J. Gen. Virol. 70 (Pt 3), 625–637.

Fry, E.E., Lea, S.M., Jackson, T., Newman, J.W.I., Ellard, F.M., Blakemore, W.E., Abu-Ghazaleh, R., Samuel, A., King, A.M.Q., Stuart, D.I., 1999. The structure and function of a foot-and-mouth disease virus-oligosaccharide receptor complex. EMBO J. 18 (3), 543–554.

Fry, E.E., Newman, J.W.I., Curry, S., Najjam, S., Jackson, T., Blakemore, W., Lea, S.M., Miller, L., Burman, A., King, A.M.Q., Stuart, D.I., 2005. Structure of FMDV serotype

$A1O_{61}$ alone and complexed with oligosaccharide receptor, receptor conservation in the face of antigenic variation. J. Gen. Virol. 86, 1909–1920.
Gromm, J.R., Hilemann, R.E., Caldwell, E.E.O., Weiler, J.M., Linhardt, R.J., 1995. Differences in the interaction of heparin with arginine and lysine and the importance of these basic amino acids in the binding of heparin to acidic fibroblast growth factor. Arch. Biochem. Biophys. 323, 279–287.
Herrera, M., García-Arriaza, J., Pariente, N., Escarmís, C., Domingo, E., 2007. Molecular basis for a lack of correlation between viral fitness and cell killing capacity. PLoS Pathog. 3 (4), e53.
Heydrick, F.P., Wachter, R.F., Hearn, H.J., 1966. Host influence on the characteristics of Venezuelan equine encephalomyelitis virus. J. Bacteriol. 91, 2343–2348.
Hooft, R.W.W., Vriend, G., Sander, C., Abola, E.E., 1996. Errors in protein structures. Nature 381, 272–1272.
Hunter, P., 1996. The performance of southern African territories serotypes of foot and mouth disease antigen in oil-adjuvanted vaccines. Rev. Sci. Tech. 15, 913–922.
Jackson, T., Ellard, F.M., Abu-Ghazaleh, R., Brookes, S.M., Blakemore, W.E., Corteyn, A.H., Stuart, D.I., Newman, J.W.I., King, A.M.Q., 1996. Efficient infection of cells in culture by type O foot-and-mouth disease virus requires binding to cell surface heparan sulfate. J. Virol. 70, 5282–5287.
Jackson, T., Sharma, A., Ghazaleh, R.A., Blakemore, W.E., Ellard, F.M., Simmons, D.L., Newman, J.W.I., Stuart, D., King, A.M.Q., 1997. Arginine-glycine-aspartic acid-specific binding by foot-and-mouth disease viruses to the purified integrin αvß3 *in vitro*. J. Virol. 71 (11), 8357–8361.
Jackson, T., Sheppard, D., Denyer, M., Blakemore, W., King, A.M.Q., 2000. The epithelial integrin alpha-v-beta-6 iis a receptor for foot-and-mouth disease virus. J. Virol. 74 (11), 4949–4956.
Jackson, T., Ellard, F.M., Ghazaleh, R.A., Brookes, S., Blakemore, W., Corteyn, A., Stuart, D., Newman, J.W.I., King, A.M.Q., 2001. Efficient infection of cells in culture by type O FMDV requires binding to cell surface heparan sulfate. J. Virol. 70, 5282–5287.
Jackson, T., Mould, A.P., Sheppard, D., King, A.M.Q., 2002. Integrin αvβ1 is a receptor for foot-and-mouth disease virus. J. Virol. 76, 935–941.
Jackson, T., Clarck, S.J., Berryman, S., Burman, A., Cambier, S., Mu, D., Nishimura, S., King, A.M.Q., 2004. Integrin αvβ8 functions as a receptor for Foot-and-mouth disease virus, role of the α-chain cytodomain in integrin-mediated infection. J. Virol. 78, 4533–4540.
Klimstra, W.B., Ryman, K.D., Johnston, R.B., 1998. Adaptation of Sindbis Virus to BHK cells selects for use of heparan sulfate as an attachment receptor. J. Virol. 72, 7357–7366.
Krusat, T., Streckert, H.-J., 1997. Heparin-dependent attachment of respiratory syncytial virus (RSV) to host cells. Arch. Virol. 142, 1247–1254.
Lea, S., Abu-Ghazaleh, R., Blakemore, W., Curry, S., Fry, E., Jackson, T., King, A., Logan, D., Newman, J., Stuart, D., 1995. Structural comparison of two strains of foot-and-mouth disease virus subtype O_1 and a laboratory antigenic variant G67. Structure 3, 571–580.
Leippert, M., Beck, E., Weiland, F., Pfaff, E., 1997. Point mutations within the betaG-betaH loop of foot-and-mouth disease virus O1K affect virus attachment to target cells. J. Virol. 71, 1046–1051.
Logan, D., Abu-Ghazaleh, R., Blakemore, W., Curry, S., Jackson, T., King, A., Lea, S., Lewis, R., Newman, J., Parry, N., 1993. Structure of a major immunogenic site on foot-and-mouth disease virus. Nature 362 (6420), 566–568.
Marshall, I.D., Scrivani, R.P., Reeves, W.C., 1962. Variation in the size of plaques produced in tissue culture by strains of western equine encephalitis virus. Am. J. Hyg. 76, 216–224.
Mason, P.W., Rieder, E., Baxt, B., 1994. RGD sequence of foot-and-mouth disease virus is essential for infecting cells via the natural receptor but can be bypassed by an antibody-dependent enhancement pathway. Proc. Natl. Acad. Sci. U.S.A. 91, 1932–1936.
Müller, H., Johne, R., Raue, R., Haas, B., Bätza, H.J., 2001. Persistence of FDMV and its effects on disease control strategies. Dtsch. Tierarztl. Wochenschr. 108 (12), 513–518.
Neff, S., Sa-Carvalho, D., Rieder, E., Mason, P.W., Blystone, S.D., Brown, E.J., Baxt, B., 1998. Foot-and-mouth disease virus virulent for cattle utilizes the integrin alpha(v)beta3 as its receptor. J. Virol. 72, 3587–3594.
Neff, S., Mason, P.W., Baxt, B., 2000. High-efficiency utilization of the bovine integrin $\alpha_v\beta3$ as a receptor for foot-and-mouth disease virus is dependent on the bovine $\alpha_v\beta$ subunit. J. Virol. 74, 7298–7306.
Office International des Epizooties, 2009. Manual of Diagnostic Tests and Vaccines for Terrestrial Animals 2009. Office International des Epizooties, Paris, France, Chapter 2.1.5, pp. 1–25.
Patel, M., Yanagishita, M., Roderiquez, G., Bou-Habib, D.C., Oravecz, T., Hascall, B.C., Norcross, M.A., 1993. Cell-surface heparan sulfate proteoglycan mediates HIV-1 infection of T-cell lines. AIDS Res. Hum. Retroviruses 9, 167–174.
Pay, T.W.F., Rweyemamu, M.M., O'Reilly, K.J., 1978. Experiences with Type SAT 2 foot-and-mouth disease vaccines in Southern Africa. In: XVth Conference of the Office International Des Epizzoties Permanent Commission on foot-and-mouth disease, pp. 1–25.
Preston, K.J., Owens, H., Mowat, G.N., 1982. Sources of variations encountered during the selection and production of three strains of FMD virus for the development of vaccine for use in Nigeria. J. Biol. Stand. 10, 35–45.
Racaniello, V.R., 2006. One hundred years of poliovirus pathogenesis. Virology 344 (1), 9–16.
Rieder, E., Bunch, T., Brown, F., Mason, P.W., 1993. Genetically engineered foot-and-mouth disease viruses with poly(C) tracts of two nucleotides are virulent in mice. J. Virol. 67, 5139–5145.
Rieder, E., Baxt, B., Mason, P.W., 1994. Animal-derived antigenic variants of foot-and-mouth disease virus type A_{12} have low affinity for cells in culture. J. Virol. 68 (8), 5296–5299.
Sa-Carvalho, D., Rieder, E., Baxt, B., Rodarte, R., Tanuri, A., Mason, P.W., 1997. Tissue culture adaptation of foot-and-mouth disease virus selects viruses that bind to heparin and are attenuated in cattle. J. Virol. 71, 5115–5123.
Sali, A., Blundell, T.L., 1993. Comparative protein modelling by satisfaction of spatial restraints. J. Mol. Biol. 234, 779–815.
Samuel, A.R., Knowles, N.J., 2001. Foot-and-mouth disease virus, cause of the recent crisis for the UK livestock industry. Trends Genet. 17 (8), 421–424.
Sellers, R.F., Daggupaty, S.M., 1990. The epidemic of foot-and-mouth disease in Saskatchewan, Canada, 1951–1952. Can. J. Vet. Res. 54 (4), 457–464.
Storey, P., Theron, J., Maree, F.F., O'Neill, H.G., 2007. A second RGD motif in the 1D capsid protein of a SAT1 type foot-and-mouth disease virus field isolate is not essential for attachment to target cells. Virus Res. 124, 184–192.
Summerford, C., Samulski, R.J., 1998. Membrane-associated heparin sulfate proteoglycan is a receptor for adeno-associated virus type 2 virions. J. Virol. 72, 1438–1445.
Thomson, G.R., 1995. Overview of foot and mouth disease in southern Africa. Rev. Sci. Tech. Off. Int. Epiz. 14 (3), 503–520.
Tomassen, F.H., de Koeijer, A., Mourits, M.C., Dekker, A., Bouma, A., Huirne, R.B., 2002. A decision-tree to optimise control measures during the early stage of a foot-and-mouth disease epidemic. Prev. Vet. Med. 54 (4), 301–324.
Van Rensburg, H.G., Mason, P., 2002. Construction and evaluation of a recombinant foot-and-mouth disease virus. Implications for inactivated vaccine production. Ann. N. Y. Acad. Sci. 969, 83–87.
Van Rensburg, H.G., Henry, T., Mason, P.W., 2004. Studies of genetically defined chimeras of a European type A virus and a South African Territories type 2 virus reveal growth determinants for foot-and-mouth disease virus. J. Gen. Virol. 85, 61–68.
Zhao, Q., Pacheco, J.M., Mason, P.W., 2003. Evaluation of genetically engineered derivatives of a Chinese strain of foot-and-mouth disease virus reveals a novel cell-binding site which functions in cell culture and in animals. J. Virol. 77, 3269–3280.
Zibert, A., Maas, G., Strebel, K., Falk, M.M., Beck, E., 1990. Infectious foot-and-mouth disease virus derived from a cloned full-length cDNA. J. Virol. 64, 2467–2473.